J. Am. Soc. Mass Spectrom. (2016) 27:124–134
DOI: 10.1007/s13361-015-1287-7

RESEARCH ARTICLE

High-Resolution Ambient MS Imaging of Negative Ions in Positive Ion Mode: Using Dicationic Reagents with the Single-Probe

Wei Rao, Ning Pan, Xiang Tian, Zhibo Yang

Department of Chemistry and Biochemistry, University of Oklahoma, Norman, OK 73019, USA

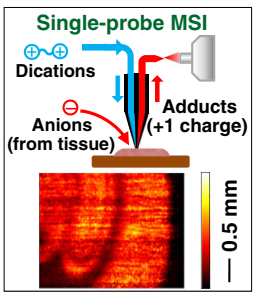

Abstract. We have used the Single-probe, a miniaturized sampling device utilizing in-situ surface microextraction for ambient mass spectrometry (MS) analysis, for the high resolution MS imaging (MSI) of negatively charged species in the positive ionization mode. Two dicationic compounds, 1,5-pentanediyl-bis(1-butylpyrrolidinium) difluoride [C_5(bpyr)$_2F_2$] and 1,3-propanediyl-bis(tripropylphosphonium) difluoride [C_3(triprp)$_2F_2$], were added into the sampling solvent to form 1+ charged adducts with the negatively charged species extracted from tissues. We were able to detect 526 and 322 negatively charged species this way using [C_5(bpyr)$_2F_2$] and [C_3(triprp)$_2F_2$], respectively, including oleic acid, arachidonic acid, and several species of phosphatidic acid, phosphoethanolamine, phosphatidylserine, phosphatidylglycerol, phosphatidylinositol, and others. In conjunction with the identification of the non-adduct cations, we have tentatively identified a total number of 1200 and 828 metabolites from mouse brain sections using [C_5(bpyr)$_2F_2$] and [C_3(triprp)$_2F_2$], respectively, through high mass accuracy measurements (mass error <5 ppm); MS/MS analyses were also performed to verify the identity of selected species. In addition to the high mass accuracy measurement, we were able to generate high spatial resolution (~17 μm) MS images of mouse brain sections. Our study demonstrated that utilization of dicationic compounds in the surface microextraction with the Single-probe device can perform high mass and spatial resolution ambient MSI measurements of broader types of compounds in tissues. Other reagents can be potentially used with the Single-probe device for a variety of reactive MSI studies to enable the analysis of species that are previously intractable.

Keywords: Single-probe mass spectrometry, High spatial resolution mass spectrometry imaging, Ambient mass spectrometry imaging, Liquid surface microextraction, Dicationic compounds, Paired ion electrospray ionization

Received: 19 August 2015/Revised: 28 September 2015/Accepted: 30 September 2015/Published Online: 21 October 2015

Introduction

Mass spectrometry imaging (MSI) is a growing field within mass spectrometry (MS) based biological analysis for the elucidation of spatially defined MS information from biological surfaces, and has already shown potential to be used in improving biomarker discovery for clinical diagnoses [1–3]. Ambient MSI describes the performance of MS analysis in the ambient environment without the need for a vacuum chamber for sampling [4], and the first description of ambient MSI was made by Takats et al. with the use of desorption electrospray ionization (DESI) MS [5]. Since then, a great number of other ambient MSI modalities have been made with a variety of different approaches [6]. Compared with non-ambient MSI techniques, such as matrix assisted laser desorption ionization (MALDI) MS [7] and time-of-flight secondary ion MS (Tof-SIMS) [8], ambient MSI methods generally lack spatial resolution, with experiments routinely performed at 50–200 μm pixel sizes or larger [9, 10]. In contrast, MALDI MS is capable of around 5 μm resolution [9], and Tof-SIMS can achieve submicron levels of precision [8] and perform depth profiling MSI on biological tissues [11]. Ambient MSI, however, has the advantage that analysis can be performed with little to no sample preparation and sampling can be conducted without a vacuum environment, allowing MSI experiments to be performed at a near native

Electronic supplementary material The online version of this article (doi:10.1007/s13361-015-1287-7) contains supplementary material, which is available to authorized users.

Correspondence to: Zhibo Yang; *e-mail:* zhibo.yang@ou.edu

state while minimizing the amount of potential artifacts within the results.

A number of ambient MSI techniques have been developed for improved MS image generation from biological samples. These ambient MSI methods can be broadly separated into a number of categories based on their principles of sampling and ionization approaches. Laser-based techniques such as laser assisted electrospray ionization (LAESI) MSI [12] and transmission geometry laser ablation MSI [13] are relatively recent developments. Both methods involve the ablation of analytes from the sample using a laser followed by ionization via ESI mechanics, and they are able to generate spatial resolutions on biological surfaces of around 30 [14] and 50 μm, respectively, with LAESI also being able to perform high throughput quantitative analysis on biological samples [15]. Spray-based techniques such as DESI MSI rely on the use of a pneumatically directed electrospray mist to desorb and ionize analytes on surfaces [16]. DESI MSI has already been successfully applied for the analysis of many different biological samples [17–19]. DESI MSI has been reported to be able to achieve a spatial resolution of up to 40 μm [20], but it is routinely performed at 100 μm or more because of experimental requirements. A growing category of ambient MSI involves in-situ surface microextraction of analytes, which has been shown to have better extraction efficiency on surfaces, such as for digested proteins, than DESI MS [21]. Some earlier examples of surface microextraction techniques include liquid micro-junction surface sampling (LMJ-SSP) MS [22, 23], which uses a coaxial probe for continuous sample uptake, and liquid extraction surface analysis (LESA) MS [24], which suspends a droplet of solvent onto the surface before taking it up for analysis via ESI-MS. Both LMJ-SSP and LESA provide surface extraction efficiency and sensitivity but are not routinely used for MSI because of a lack of spatial resolution (typically 0.5–1.0 mm), and they are usually used for profiling biomolecules on surfaces [25–27]. Nano-DESI is a surface microextraction-based technique that has shown great promise in the field of MSI. The nano-DESI probe consists of two individual fused silica capillaries placed together to form a micro-junction on a surface, which is then supplied with solvent into one of the capillaries so that extracted analytes can be taken up by the other and analyzed within the mass spectrometer [28]. Nano-DESI is capable of high spatial resolution at around 12 μm on biological samples [29] and has been used previously for a number of MSI investigations of a variety of biological tissues [30–32]; however, reproducible probe fabrication and the initial setup of the probe for optimal sample interaction can be difficult. We have created the Single-probe, an integrated sampling and ionization device that can be coupled with MS for a variety of applications. The Single-probe works via surface microextraction, and is capable of high spatial resolution ambient MSI [33] as well as a number of other modalities such as live single cell MS analysis [34]. The Single-probe is constructed using a pulled dual-bore quartz tubing coupled to two fused silica capillaries for solvent introduction and aspiration, which allows the device to have an integrated structure, small sampling size, high extraction efficiency, and convenient operation for ambient MSI measurements. In particular, the smallness of the probe tip size (typically <10 μm) allows for sampling to be conducted at a small area. We were able to achieve a spatial resolution of around 8.5 μm on mouse kidney sections in our previous work, which is amongst the highest spatial resolutions yet achieved using ambient MSI techniques on biological tissues [33].

All ambient MSI techniques mentioned above (i.e., DESI, LASESI, LMJ-SSP, LESA, and nano-DESI) are relevant to the ESI method. Because negative ionization mode has been shown to be generally less sensitive and stable than the positive ionization mode for most molecular species due to the increased tendencies for corona discharging in the negative ionization mode [35], these ambient MSI techniques are generally operated under the positive ionization mode. The development of ESI techniques, such as varying the solvent composition, is expected to expand the capabilities of these ambient MSI methods. In addition to the use of common solvents (e.g., methanol, water, and acetonitrile), reagents containing solvent can be used in ESI-MS techniques to improve the detection of certain metabolites [36, 37]. For example, dicationic compounds have been used as reagents to improve the detection of phospholipids in LC-MS experiments [38]. These dicationic compounds carry 2+ charge and readily form adducts with negatively charged (1−) species such as phospholipids; the formation of 1+ charged adducts allows the detection of anionic species in the positive ionization mode [39]. Similarly, this method has already been employed in the analysis of a number of negatively charged pesticides using high performance liquid chromatography (HPLC) ESI MS (termed paired ion ESI (PIESI)), and was found to have improved the sensitivity of detection of their target compounds [40]. In addition to the ESI-MS experiments, dicationic compounds have been applied for ambient surface analyses. A number of dicationic compounds were used in DESI MS for the detection of stock lipid species spotted onto a glass surface, where one of the dicationic compounds $[C_6(C_1Pyrr)_2][Br]_2$ was show to have selectively improved the detection of palmitoleic acid and linoleic acid over their detection in the negative ionization mode [41]. $[C_6(C_1Pyrr)_2][Br]_2$ was later applied to DESI MSI studies on biological tissues, where adducts of dicationic compound with fatty acids in the range of *m/z* 250−350 were observed in the positive ionization mode [42]. However, this study was unable to observe adducts of the dicationic compound with larger phospholipids that typically exist within the range of *m/z* 600−900 within their MSI results.

Here, we present the utilization of the dicationic compounds [40] for reactive MSI experiments to obtain high spatial and mass resolution ambient MS images of biological tissues using the Single-probe device. We were able to detect a large number of negatively charged species in the positive ionization mode with both dicationic compounds, mostly in the *m/z* 600–900 range, including many species of phosphatic acids (PA), phosphoethanolamines (PE), phosphatidylglycerol (PG), phosphatidylserine (PS), phosphatidylinositol (PI), and others.

Metabolites normally found in the positive ionization mode were also simultaneously detected during these experiments. Considering that the same sample slice usually is not reused for additional measurements in all MSI studies because of sample destruction or analyte depletion, some chemical information cannot be obtained in one experiment using either positive or negative MS polarity. Combined with the detection of the dicationic compound adducts in the same experiment, our technique can greatly increase the total number of identifications through one experiment. The dicationic compounds were able to improve the spectral intensities of the ions detected over the negative mode as well. The Single-probe MSI experiments can be carried out using high-resolution mass spectrometers, such as Thermo (Waltham, MA, USA) LTQ Orbitrap XL mass spectrometer, allowing for a confident identification of the species than previously achieved [42]. MS/MS was also performed on selected ions to further improve the identification. We were able to achieve a spatial resolution of 17 µm for both of the dicationic compounds on the mouse brain section samples. Our results indicate that dicationic reagents can improve solvent-based ambient MSI experiments and enable a greater number of molecular species to be imaged in a single experiment, which would allow more informative analyses of the biological samples to be performed.

Experimental

Chemicals

Methanol and water (Chromasolv MS grade) were purchased from Sigma-Aldrich (St. Louis, MO, USA). Two dicationic compounds, 1,5-pentanediyl-bis(1-butylpyrrolidinium) difluoride (the dication is abbreviated to $[C_5(bpyr)_2]^{2+}$) and 1,3-propanediyl-bis(tripropylphosphonium) difluoride (the dication is abbreviated to $[C_3(triprp)_2]^{2+}$, which were first described in Xu and Armstrong [40], were purchased from Sigma-Aldrich (St. Louis, MO, USA) at a concentration of 2.5 mM in methanol:water (50:50) (Figure 1). These dicationic compounds were used to prepare a series of concentrations from 10 µM to 1 mM with the solvent methanol:water at a composition of 90:10.

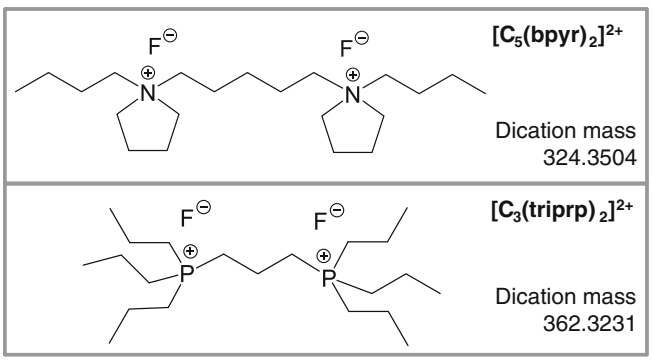

Figure 1. Structures of the dicationic compounds ($[C_5(bpyr)_2]^{2+}$ and $[C_3(triprp)_2]^{2+}$) used in Single-probe MSI experiments. The masses of the dication portion of the molecules are also presented

Preparation of Brain Section

Mouse brain tissues were placed in Optimum Cutting Temperature (OCT) compound (Tissue-Tek, Sakura Finetek USA, Torrance, CA) and flash-frozen in liquid nitrogen before sectioning within a cryotome (American Optical 845 Cryo-cut Microtome, Southbridge, MA, USA) at −15°C. The brain sections were made at 12 µm thickness and placed onto polycarbonate microscope slides (P11011P; Science Supply Solutions, Elk Grove Village, IL, USA). Samples were dried in the open air, scanned at high resolution using a PathScan Enabler IV histology slide scanner (Meyer Instruments, Inc., Houston, TX, USA), and stored at –80°C before use.

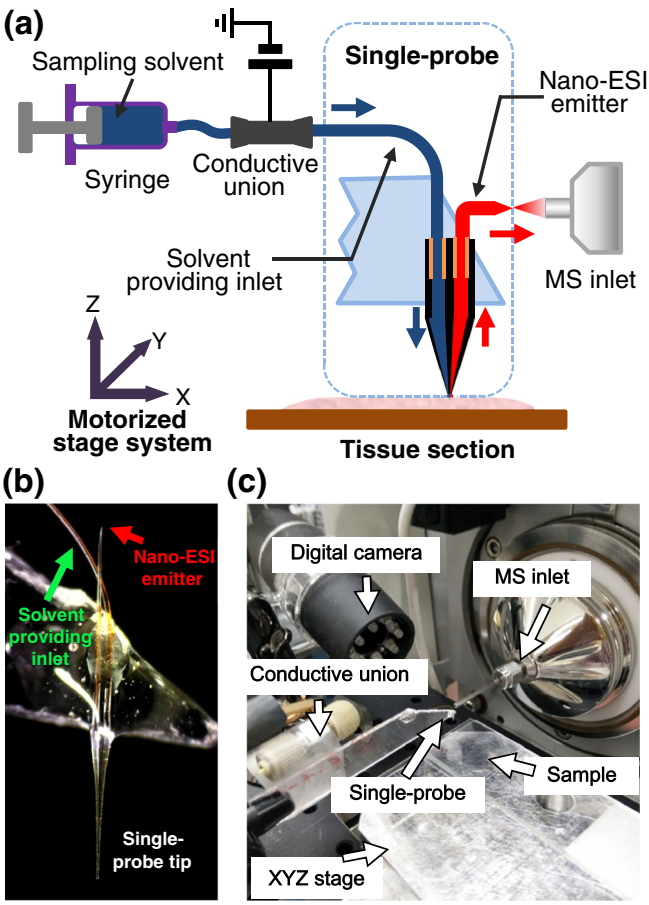

Figure 2. (**a**) Schematic representation of the Single-probe setup. Presented are the structure of the Single-probe with the solvent providing inlet and the nano-ESI emitter. A liquid junction formed between the probe tip and the tissue section allows for surface extraction, and the extracted analytes are drawn towards the nano-ESI emitter for MS analysis. The syringe provides the sampling solvent while the conductive union transmits the ionization voltage. (**b**) Photo of a fabricated Single-probe. (**c**) Photo showing the components of the Single-probe MSI setup

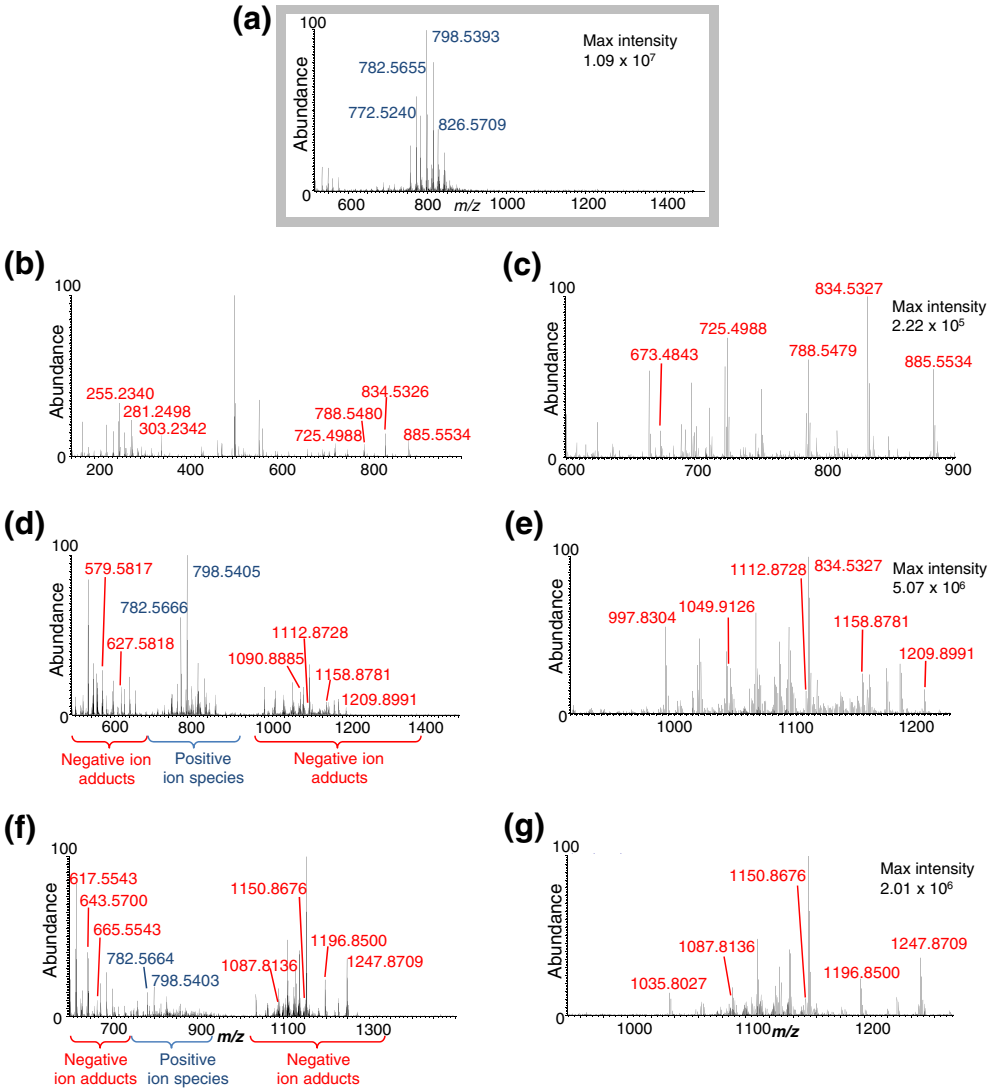

Figure 3. Mass spectra of MS analyses of mouse brain sections. (**a**) Typical mass spectrum obtained in the positive ionization mode (no dicationic reagents) shown in the *m/z* 600–900 range. (**b**) Typical mass spectrum in the negative ionization mode; details within *m/z* 600–900 range are shown in (**c**). (**d**) Mass spectrum in the positive ionization mode with 400 μM solution of $[C_5(bpyr)_2]^{2+}$, including regions of normal positive ions and negative ion adducts; details within *m/z* 925–1225 range are shown in (**e**). (**f**) Mass spectrum in the positive ionization mode with 400 μM solution of $[C_3(triprp)_2]^{2+}$, including regions of normal positive ions and negative ion adducts; details within *m/z* 950–1250 range are shown in (**g**)

Fabrication of the Single-probe

The Single-probe (Figure 2a and b) fabrication was described in detail in previous publications [33, 34]. Briefly, the device was made from a dual-bore quartz tubing (outer diameter (o.d.) 500 μm; inner diameter (i.d.) 127 μm; Friedrich and Dimmock, Inc., Millville, NJ, USA) pulled to a fine needle using a Sutter P-2000 laser puller (Sutter Instrument, Novato, CA, USA). Two fused silica capillaries (o.d. 105 μm, i.d. 40 μm; Polymicro Technologies, Phoenix, AZ, USA) were placed inside each channel within the pulled dual-bore quartz needle at the flat end, sealed with UV activated bonding resin (Light Cure Bonding Adhesive; Prime-Dent, Chicago, Il, USA), and the whole device was then secured onto a glass slide using regular epoxy. One of

Table 1. Number of Metabolites Tentatively Identified on Mouse Brain Section (Mass Error <5 ppm)

Ionization mechanism[a]	Anions[b]	Cations[c]	Total[d]
−ve	576	N/A	576
+ve with $[C_5(bpyr)_2]^{2+}$	526 (163)	674	1200
+ve with $[C_3(triprp)_2]^{2+}$	322 (87)	506	828

[a]Ionization mechanisms used, including the regular negative ionization mode (−ve) and positive ion mode (+ve) with $[C_5(bpyr)_2]^{2+}$ or $[C_3(triprp)_2]^{2+}$
[b]Number of identified anions; numbers in parentheses indicate the common species identified using the regular negative ion mode
[c]Number of identified cations
[d]Total number of identified metabolites. For a list of the metabolites please refer to Supplementary Tables S1–S5

the fused silica capillaries acts as the solvent providing inlet whereas the other plays the role as the nano-ESI emitter (Figure 2b). The Single-probe device has been coupled with a XYZ translation stage system for sample motion control and a Thermo LTQ Orbitrap XL mass spectrometer for MS analysis (Figure 2a and c).

MSI Experiment and Data Processing

A mouse brain section was placed onto a motorized XYZ stage system controlled by a LabVIEW software developed by the Laskin Group [43]. MSI was performed on a Thermo LTQ Orbitrap XL mass spectrometer with the following parameters: 10.0 μm/s rastering speed and 20 μm distance between lines, mass resolution 60,000 (m/Δm), 5 kV positive mode, 1 microscan, 100 ms max injection time, AGC on. It is noted that compared with conventional ESI-MS settings, a relatively higher ionization voltage was used in our experiments, whereas no corona discharging was observed on the nano-ESI emitter. Owing to the smallness of the nano-ESI emitter (length ~5 mm) on the Single-probe device, the ionization voltage is conveniently applied on the conductive union, and then transmitted to the nano-ESI emitter through the liquid in the capillaries and channels in the Single-probe (Figure 2a). It is very likely that a voltage drop occurs during the voltage transmission, and the actual ionization voltage applied onto the nano-ESI emitter is significantly reduced. Solvents used for dicationic compound reactive imaging were methanol:water (90:10) containing $[C_5(bpyr)_2]^{2+}$ or $[C_3(triprp)_2]^{2+}$ at a number of concentrations with a flow rate of 0.4 μL/min. With this flow rate, solvent delivered to the surface can be completely drawn up by the ESI-emitter with no surface spreading observed. The total time for a typical high resolution MSI experiment for a sample of 2.0 × 1.5 mm in size is around 4–5 h. MS images were generated from raw data files using the MSI QuickView software developed by PNNL [44]. Accurate mass of metabolite was searched using the online database Metlin from the Scripps Center for Metabolomics (https://metlin.scripps.edu/index.php).

MS/MS of Selected Ions

For more confident identification of species of interest, spot surface analyses of metabolites on mouse brain sections were carried out using MS/MS with collision induced dissociation (CID) and/or higher-energy collision-activated dissociation (HCD). HCD MS/MS was performed for the selected species (in the negative ionization mode for comparison) and the adducts of metabolites with dicationic compounds $[C_5(bpyr)_2]^{2+}$ and $[C_3(triprp)_2]^{2+}$. The parameters used in MS/MS analyses were as follows: mass resolution 100,000 (m/Δm), 5 kV positive mode for dicationic experiments and negative mode for control, 1 microscan, 100 ms injection time, AGC on, activation type CID or HCD, isolation width *m/z* 1.0 (*m/z* ±0.5 window), normalized collision energy 30 (manufacturer's unit) for both CID and HCD.

Results and Discussion

Detection of Negatively Charged Species in the Positive Ionization Mode Using Dicationic Compounds

Ambient MSI techniques utilizing solvents for sampling or ionization (e.g., LAESI [45], DESI [46], nano-DESI [30], and LMJ-SSP [27]) are usually conducted either in the positive or negative ionization mode, depending on the polarities of a specific subset of metabolites. In the positive ionization mode a large number of phosphatidylcholine (PC), phosphoethanolamine (PE), and sphingomyelin (SM) are observed around the *m/z* 600–900 range, whereas in the negative ionization mode a greater range of phospholipids, such as PEs, phosphatic acid (PA), phosphatidylglycerol (PG), phosphatidylserine (PS), phosphatidylinositol (PI), and others can be detected [47]. Typically, it is found that in ESI-MS experiments, positive ionization mode provides better sensitivity and stability than the negative ionization mode, which exhibits an increased tendency for corona discharging [35]. It was our goal in these studies to use the solvent containing dicationic compounds to enable the detection of negatively charged metabolites in the positive ionization mode of the mass spectrometer, and increase the amount of metabolites to be observed within a single MSI experiment.

We first conducted spot MS analyses of metabolites from mouse brain sections using the Single-probe in both positive and negative ionization modes. Figure 3a and b are the representative spectra that can be observed from the surface of a mouse brain section in the positive and negative ionization modes, respectively. It is worth noting that the phospholipids in both spectra reside within the *m/z* 600–900 range, shown for the negative ionization mode in Figure 3c. The dicationic compounds, either $[C_5(bpyr)_2]^{2+}$ or $[C_3(triprp)_2]^{2+}$ (Figure 1), were added into the sampling solvent in the syringe for surface microextraction of analytes. Typical MS spot analysis spectra obtained using these two dicationic compounds are shown in Figure 3d and f. For $[C_5(bpyr)_2]^{2+}$ the negatively charged metabolites form adducts with the dicationic ligand, with a mass shift of *m/z* 324.3504, which can be seen in the *m/z* 925–1225 range (Figure 3e). Similarly, for $[C_3(triprp)_2]^{2+}$ the negatively charged metabolites associate with the dicationic ligand, with a mass shift of *m/z* 362.3231, which formed the complexes that can be observed in the *m/z* 950–1250 range (Figure 3g). Metabolites normally observed in the positive ionization mode can still be detected in their usual *m/z* values (*m/z* 600–900) while using the dicationic reagents (Figure 3d and f).

The sampling solutions at a series of concentrations for both dicationic compounds were tested from 10 μM to 1 mM, and an optimal concentration of 400 μM was used for the Single-probe MSI experiments. This concentration is higher than those used in previous LC-PIESI MS (40 μM) [40] and DESI-MS (10 μM) [41] studies. It is likely that in our MSI experiments, a larger amount of complex molecules extracted from biological

tissues can form adducts with the dicationic compounds resulting in higher consumptions of dicationic reagents. A potential disadvantage resulting from such a high concentration of dicationic reagent is likely to be the ionization suppression of certain types of analytes. This was observed for $[C_3(triprp)_2]^{2+}$ where the non-adduct cations have their absolute ion intensities generally lower than those in the experiments without using the dicationic reagents (Table 1, Figure 3a and f). However, the ion suppression effect was unlikely to be present for $[C_5(bpyr)_2]^{+}$, where the intensities for non-adduct cations were not affected (Figure 3a and d). In addition, due to the complexity of mass spectrum obtained from this reactive MSI experiments, using high resolution mass spectrometer is necessary to acquire detailed chemical information of tissue samples.

Single-probe Ambient MSI with Dicationic Compounds

MSI experiments of mouse brain sections were performed using the Single-probe MSI setup with both of the dicationic compounds $[C_5(bpyr)_2]^{2+}$ (Figure 4) and $[C_3(triprp)_2]^{2+}$ (Figure 5). A representative metabolite that is commonly found in the positive ionization mode [PC (34:1)] is also observed for each of the reactive MS images (Figure 4b and Figure 5b). MS images of a selection of metabolites adducted with each of the dicationic compounds, including docosahexaenoic acid (DA) (22:6), PA (36:1), PE (P-38:6), PG (34:1), PS (40:6), and PI (38:4), are presented in Figure 4c and Figure 5c, respectively. The detection of these phospholipids in the *m/z* 600–900 is an improvement over previous results from DESI MSI where these metabolites were not detected with the application of a different dicationic compound [42]. The number of scans per line of raster was 301 scans in 260 s for both of the MSI measurements, and features within the tissues could be clearly seen in these MS images. The spatial resolution for the MS images was determined using changes in the intensity of the MS spectra around these features as suggested previously [48], which was found to be 17 μm (pixel size 17 × 20 μm, across two MS measurements) based on the ion intensity change of the peak fount at $[PA\ (36:1) - H + C_5(bpyr)_2]^{+}$ (*m/z* 1025.8651) and $[PA\ (36:1) - H + C_3(triprp)_2]^{+}$ (*m/z* 1063.8328) at three different points for both of the dicationic compound MS images, respectively (Supplementary Figures S1 and S2). These

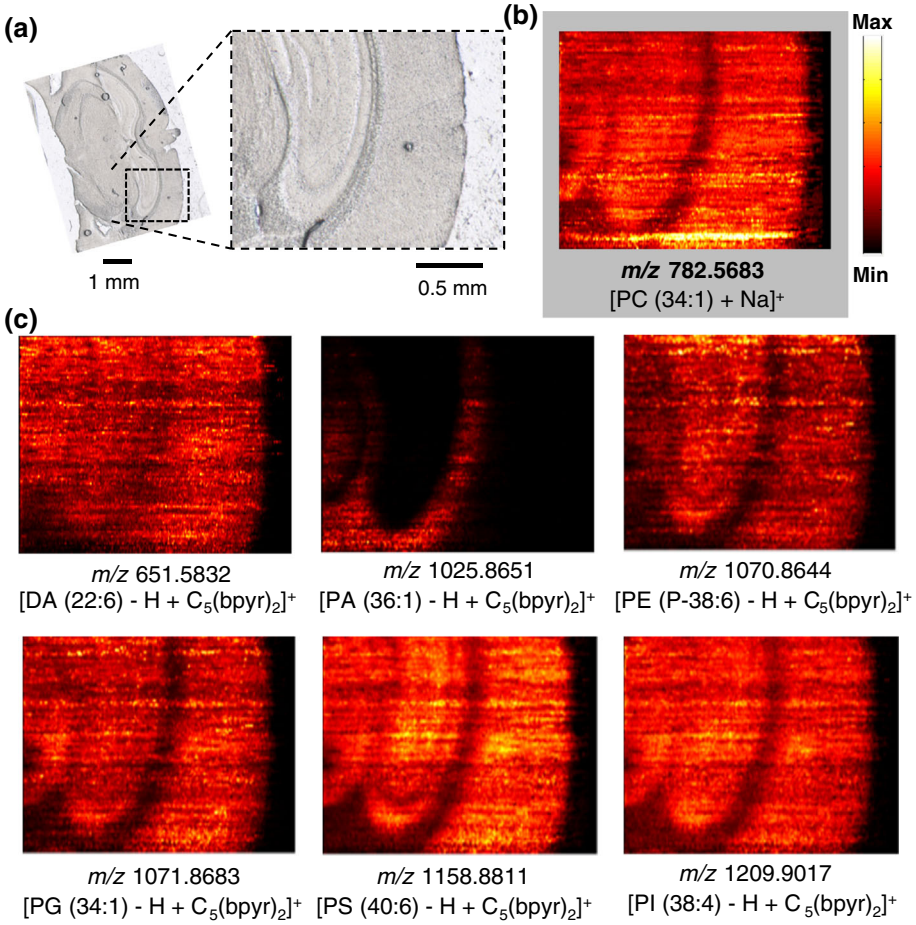

Figure 4. The Single-probe MSI results obtained using $[C_5(bpyr)_2]^{2+}$ species. (**a**) Optical image of the mouse brain section used for MSI. (**b**) MS image of $[PC\ (34:1) + Na]^{+}$, an ion normally found in the positive ionization mode. (**c**) MS images of dicationic adducts, including $[DA\ (22:6) - H + C_5(bpyr)_2]^{+}$, $[PA\ (36:1) - H + C_5(bpyr)_2]^{+}$, $[PE\ (P\text{-}38:6) - H + C_5(bpyr)_2]^{+}$, $[PG\ (34:1) - H + C_5(bpyr)_2]^{+}$, $[PS\ (40:6) - H + C_5(bpyr)_2]^{+}$, and $[PI\ (38:4) - H + C_5(bpyr)_2]^{+}$

images were obtained with a slightly lower spatial resolution than previously achieved using the Single-probe (8.5 μm) without the addition of dicationic compounds [33]. The reduced spatial resolution in the current study is possibly due to the slightly increased carryover of the dicationic adducts within the probe during the MSI experiments. Nevertheless, the spatial resolution is still generally high amongst all ambient MSI experimental results conducted on biological tissue samples. The carryover issues of the dicationic compounds can be potentially improved in the future via systematic trials, including using different dicationic compounds, optimizing the reagent concentration and flow rate, and choosing the fused silica capillaries with smaller i.d. to produce the nano-ESI emitters with smaller dead-volume for the Single-probe.

Metabolite Identification with High Accurate Mass MS

The capabilities of the Thermo LTQ Orbitrap XL mass spectrometer enable us to perform high accurate mass analysis to identify metabolites on tissue surfaces. Spot analyses on mouse brain sections were performed in the negative ion mode and in the positive mode with $[C_5(bpyr)_2]^{2+}$, and $[C_3(triprp)_2]^{2+}$ added in to the sampling solvent. All of the metabolites were tentatively identified using MS measurements with high mass accuracy (mass error <5 ppm) for the matched molecular formulas. Overall, 576 species were tentatively labeled in the negative ionization mode (Table 1, for full list refer to Supplementary Table S1), which includes many phospholipids that were identified in the *m/z* 600–900 range (Figure 3a). For experiments using $[C_5(bpyr)_2]^{2+}$, a total of 526 negatively charged metabolites were tentatively labeled after the subtraction of the dication's mass shift (*m/z* 324.3504) from each peak (Table 1, for full list refer to Supplementary Table S2). Among these 526 identified species, 163 were also detected in the negative ionization mode. $[C_5(bpyr)_2]^{2+}$ was able to form adducts with a broad range of negatively charged metabolites, and this dication does not seem to favor any particular mass range. This observation is in contrast with previous DESI-MSI studies, in which dicationic compound $[C_6(C_1Pyrr)_2][Br]_2$ [41, 42] was chosen as the reagent, where the higher mass ranges were less well detected. It is very likely that the difference of detection range resulted from the difference of sampling and ionization mechanisms between the Single-probe MSI and DESI-MSI techniques. For example, DESI has been shown to be generally less sensitive for the detection of high molecular weight species [21].

In particular, we were able to detect some biologically important metabolites, such as adenosine monophosphate (AMP, $C_{10}H_{14}N_5O_7P$), which were not detected in the negative

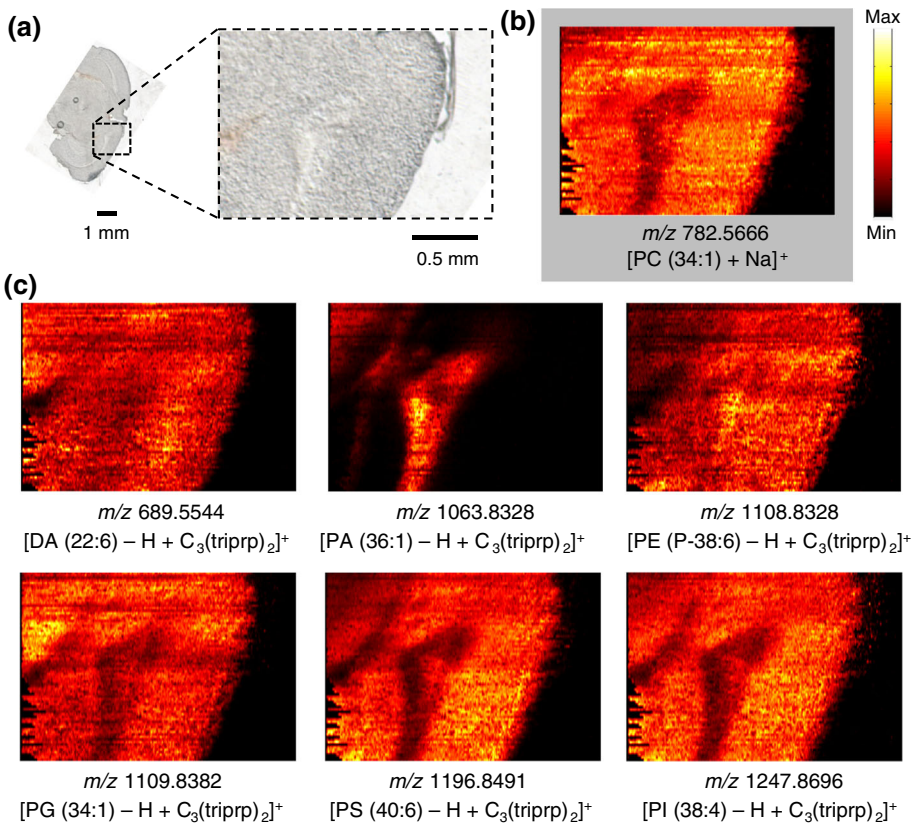

Figure 5. The Single-probe MSI results obtained using $[C_3(triprp)_2]^{2+}$ species. (**a**) Optical image of the mouse brain section used for MSI. (**b**) MS image of [PC (34:1) + Na]$^+$, an ion normally found in the positive ionization mode. (**c**) MS images of dicationic adducts, including [DA (22:6) – H + $C_3(triprp)_2]^+$, [PA (36:1) – H + $C_3(triprp)_2]^+$, [PE (P-38:6) – H + $C_3(triprp)_2]^+$, [PG (34:1) – H + $C_3(triprp)_2]^+$, [PS (40:6) – H + $C_3(triprp)_2]^+$, and [PI (38:4) – H + $C_3(triprp)_2]^+$

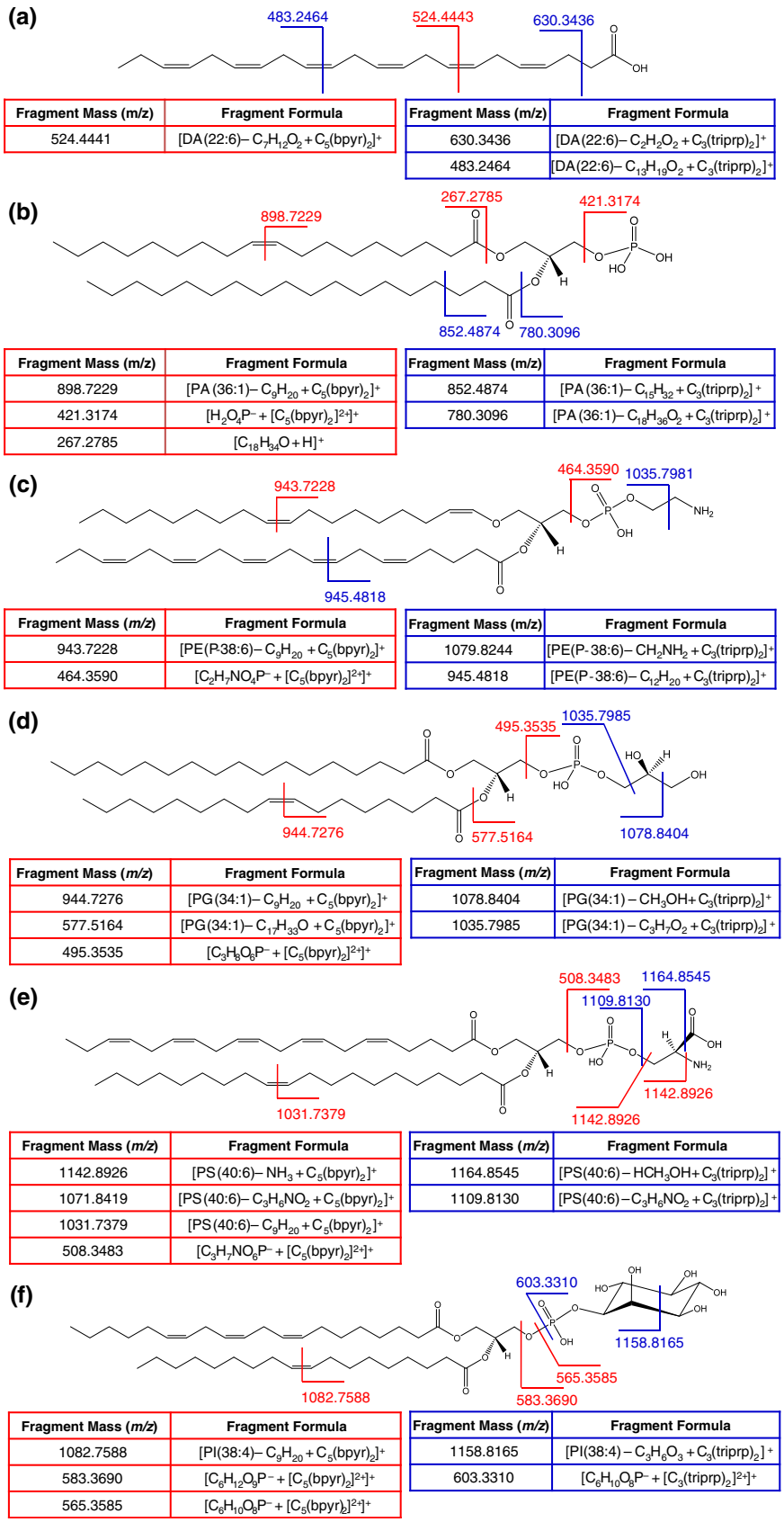

Fragment Mass (m/z)	Fragment Formula
524.4441	[DA(22:6)– $C_7H_{12}O_2$ + $C_5(bpyr)_2]^+$

Fragment Mass (m/z)	Fragment Formula
630.3436	[DA(22:6)– $C_2H_2O_2$ + $C_3(triprp)_2]^+$
483.2464	[DA(22:6)– $C_{13}H_{19}O_2$ + $C_3(triprp)_2]^+$

Fragment Mass (m/z)	Fragment Formula
898.7229	[PA (36:1)– C_9H_{20} + $C_5(bpyr)_2]^+$
421.3174	[$H_2O_4P^-$ + $[C_5(bpyr)_2]^{2+}]^+$
267.2785	[$C_{18}H_{34}O$ + H]$^+$

Fragment Mass (m/z)	Fragment Formula
852.4874	[PA (36:1)– $C_{15}H_{32}$ + $C_3(triprp)_2]^+$
780.3096	[PA (36:1)– $C_{18}H_{36}O_2$ + $C_3(triprp)_2]^+$

Fragment Mass (*m/z*)	Fragment Formula
943.7228	[PE(P-38:6)– C_9H_{20} + $C_5(bpyr)_2]^+$
464.3590	[$C_2H_7NO_4P^-$ + $[C_5(bpyr)_2]^{2+}]^+$

Fragment Mass (m/z)	Fragment Formula
1079.8244	[PE(P-38:6)– CH_2NH_2 + $C_3(triprp)_2]^+$
945.4818	[PE(P-38:6)– $C_{12}H_{20}$ + $C_3(triprp)_2]^+$

Fragment Mass (*m/z*)	Fragment Formula
944.7276	[PG(34:1)– C_9H_{20} + $C_5(bpyr)_2]^+$
577.5164	[PG(34:1)– $C_{17}H_{33}O$ + $C_5(bpyr)_2]^+$
495.3535	[$C_3H_8O_6P^-$ + $[C_5(bpyr)_2]^{2+}]^+$

Fragment Mass (*m/z*)	Fragment Formula
1078.8404	[PG(34:1) – CH_3OH+ $C_3(triprp)_2]^+$
1035.7985	[PG(34:1) – $C_3H_7O_2$ + $C_3(triprp)_2]^+$

Fragment Mass (*m/z*)	Fragment Formula
1142.8926	[PS(40:6)– NH_3 + $C_5(bpyr)_2]^+$
1071.8419	[PS(40:6)– $C_3H_6NO_2$ + $C_5(bpyr)_2]^+$
1031.7379	[PS(40:6)– C_9H_{20} + $C_5(bpyr)_2]^+$
508.3483	[$C_3H_7NO_6P^-$ + $[C_5(bpyr)_2]^{2+}]^+$

Fragment Mass (*m/z*)	Fragment Formula
1164.8545	[PS(40:6) – HCH_3OH+ $C_3(triprp)_2]^+$
1109.8130	[PS(40:6) – $C_3H_6NO_2$ + $C_3(triprp)_2]^+$

Fragment Mass (*m/z*)	Fragment Formula
1082.7588	[PI(38:4)– C_9H_{20} + $C_5(bpyr)_2]^+$
583.3690	[$C_6H_{12}O_9P^-$ + $[C_5(bpyr)_2]^{2+}]^+$
565.3585	[$C_6H_{10}O_8P^-$ + $[C_5(bpyr)_2]^{2+}]^+$

Fragment Mass (*m/z*)	Fragment Formula
1158.8165	[PI(38:4) – $C_3H_6O_3$ + $C_3(triprp)_2]^+$
603.3310	[$C_6H_{10}O_8P^-$ + $[C_3(triprp)_2]^{2+}]^+$

Figure 6. MS/MS analyses of selected adducts with $[C_5(bpyr)_2]^{2+}$ (in red) and $[C_3(triprp)_2]^{2+}$ (in blue). Shown are the chemical structures of the molecules, the position of fragmentation, and tables summarizing the *m/z* of the fragment and the corresponding molecular formula for (**a**) DA (22:6), (**b**) PA (36:1), (**c**) PE (P-38:6), (**d**) PG (34:1), (**e**) PS (40:6), and (**f**) PI (38:4)

ion mode. The peak intensities of the $[C_5(bpyr)_2]^{2+}$ adducts were much higher than those that can be achieved in the negative ionization mode, with more than 25 times higher intensity observed for the most abundant peak in the phospholipid mass range (Figure 3c and e). In addition to the negative metabolites detected, 674 non-adduct cations were tentatively labeled in the positive ionization mode, such that a total of 1200 metabolites were tentatively identified (Table 1, for full list refer to Supplementary Table S3). The identified positive ions were predominantly found in the *m/z* 600–900 range of the positive ionization mode, with relatively fewer identified in the mass shifted *m/z* 925–1225 range of the $[C_5(bpyr)_2]^{2+}$ adducted ions.

For MSI experiments using $[C_3(triprp)_2]^{2+}$, a total of 322 negatively charged metabolites were tentatively identified with the subtraction of the dications mass shift (*m/z* 362.3231) from each peak within the spectrum (Table 1, for full list refer to Supplementary Table S4). Among 322 identified species, 87 were also detected in the negative ionization mode. Although $[C_3(triprp)_2]^{2+}$ can form adducts with a broad range of metabolites found in the negative ionization mode, the signal intensities of these adducts were relatively lower than those of $[C_5(bpyr)_2]^{2+}$ adducts. It is likely that in $[C_3(triprp)_2]^{2+}$ the shorter linker chain between the two cationic centers may sterically hinder adduct formation compared with $[C_5(bpyr)_2]^{2+}$ (Figure 2). Nevertheless, $[C_3(triprp)_2]^{2+}$ can still produce spectral intensities at around nine times of those observed in the negative ionization mode (Figure 3c and g). Using $[C_3(triprp)_2]^{2+}$ as the reagent, we were also able to detect AMP as an adduct of the negative ion. Particularly, this dication allows for selective detection of a number of triglycerides (TG) at the mass range of *m/z* 950 to 1100 that were not detected in either the negative ionization mode or with $[C_5(bpyr)_2]^{2+}$. It follows that $[C_3(triprp)_2]^{2+}$ can potentially be used to selectively enhance the detection of a class of molecules that previously were unable to be detected in the negative ionization mode. In addition to the detection of adducts with negatively charged metabolites, 506 non-adduct cations were also observed, indicating that around 828 metabolites were tentatively identified in total (Table 1, for full list refer to Supplementary Table S5). The total number of detected metabolites is less than that observed with $[C_5(bpyr)_2]^{2+}$, which could be due to a lesser degree of ion intensity enhanced by the $[C_3(triprp)_2]^{2+}$ reagent. Nevertheless, $[C_3(triprp)_2]^{2+}$ was still able to detect a larger number of metabolites than can be found in the negative ionization mode alone without using the dicationic compound.

MS/MS Analysis of Metabolites Adducted with Dicationic Compounds

The combination of accurate MS measurement with standard database search, such as Metlin, is commonly used for the identifications of metabolites. However, because of the achievable mass accuracy (mass error <5 ppm) in our experiments, it is still possible to obtain false positives, particularly for large species. Owing to the lack of the fragment information of dication adducts investigated in the current study in any database, we have conducted accurate-mass MS/MS analysis of selected metabolites to elucidate the general fragmentation rules and to obtain further identification of these adducts. The lipid species DA (22:6), and the phospholipid species PA (36:1), PE (P-38:6), PG (34:1), PS (40:6), and PI (38:4) were subjected to CID and HCD MS/MS for both of the dicationic species, as they represent a broad selection of the kinds of lipids that were found on the surface. For the MS/MS analysis of DA (22:6) adducts, the fragmentation of both the $[C_5(bpyr)_2]^{2+}$ and $[C_3(triprp)_2]^{2+}$ adducts proceed through the neutral losses ($C_2H_2O_2$) from the carboxylic acid group (Figure 6, Supplementary Figure S3a).

For the phospholipids, fragments containing the headgroups (1– charged) were observed for all their adducts with $[C_5(bpyr)_2]^{2+}$, yielding $[\text{headgroup} + [C_5(bpyr)_2]^{2+}]^+$ ions (i.e., PA(36:1) − $[H_2O_4P^- + [C_5(bpyr)_2]^{2+}]^+$, *m/z* 421.3174; PE (P-38:6) − $[C_2H_7NO_4P^- + [C_5(bpyr)_2]^{2+}]^+$, *m/z* 464.3590; PG (34:1) − $[C_3H_8O_6P^- + [C_5(bpyr)_2]^{2+}]^+$, *m/z* 495.3535; PS (40:6) − $[C_3H_7NO_6P^- + [C_5(bpyr)_2]^{2+}]^+$, *m/z* 508.3483; and PI (38:4) − $[C_6H_{10}O_8P^- + [C_5(bpyr)_2]^{2+}]^+$, *m/z* 565.3585; Figure 6b–f) that were detected within the MS/MS spectra (Supplementary Figure S3b–f). The detection of these $[\text{Headgroup} + [C_5(bpyr)_2]^{2+}]^+$ ions indicates that the dicationic compound was able to form a relatively stronger electrostatic interaction with the negatively charged headgroups than some covalent bonds during the adduct fragmentation processes. Other fragments were also observed in the positive ionization mode, including some species without the dicationic compound.

For the phospholipids adducted with $[C_3(triprp)_2]^{2+}$, a number of fragments containing the dicationic compound were observed for above five phospholipids tested in the MS/MS experiments with $C_5(bpyr)_2]^{2+}$. However, the number of fragments observed for each of the phospholipids was generally less than their corresponding adducts with $[C_5(bpyr)_2]^{2+}$ (Figure 6b–f). The $[\text{headgroup} + [C_3(triprp)_2]^{2+}]^+$ fragment was only observed for PI (38:4) ($[C_6H_{10}O_8P^- + [C_3(triprp)_2]^{2+}]^+$, *m/z* 603.3310; Figure 6f), which was probably due to stronger hydrogen bonding between the $[C_3(triprp)_2]^{2+}$ dicationic and –OH groups in the headgroup on the PI (38:4) molecule (spectra can be found in Supplementary Figure S3b–f). These results indicate that $[C_3(triprp)_2]^{2+}$ has a generally weaker ability for forming adduct than $[C_5(bpyr)_2]^{2+}$, which may be due to its relatively shorter linker chain length hindering the stronger interactions with the relatively larger target ions. This result is different from the one Xu and Armstrong [49] observed for PIESI MS of these dicationic compounds during the detection of pesticides, where $[C_3(triprp)_2]^{2+}$ has been found to be better at signal enhancement than $[C_5(bpyr)_2]^{2+}$. This difference may have been the result that the pesticides investigated in previous studies are generally small molecules with masses below 300, whereas the dicationic compounds interact with the larger phospholipids in the current study, resulting in different affinities from those previously observed.

Conclusion

We have utilized for the first time dicationic compounds for the high spatial and mass resolution ambient MSI analysis of biological tissue surfaces with the Single-probe device. Both of the dicationic compounds, $[C_5(bpyr)_2]^{2+}$ and $[C_3(triprp)_2]^{2+}$, were able to form adducts with the negatively charged metabolites present in the samples allowing for their detection in the positive ionization mode; 526 and 322 negatively charged metabolites were tentatively identified using high accurate mass as adducts with $[C_5(bpyr)_2]^{2+}$ and $[C_3(triprp)_2]^{2+}$, respectively. The total number of metabolites found (including positively charged metabolites under normal conditions) were 1200 and 828, respectively, which is a great increase of the number of metabolites that can be identified using one MS polarity alone. A large number of the negatively charged metabolites adducted with the dications were found in the relatively high mass range of *m/z* 600−900, which is an improvement of the detection range compared with previous ambient DESI MSI of biological samples [42]. The ion intensities within the spectra were also higher for the dicationic adducts than those achieved in the negative ionization mode. In particular, the dicationic compounds were able to facilitate the detection of a number of compounds that were not detected under the negative ionization mode in MS analysis. Dicationic compounds can be made with many different designs, including compounds with asymmetric designs [50] and additional charges [38] (such as tri- and tetra-cationic compounds), which may offer improved abilities for the sensitive detection of specific metabolites or drug molecules [51]. The combination of dicationic compounds with the Single-probe MSI technique indicates that other reagents can be potentially added into the sampling solvent for reactive MSI experiments, which could offer an even greater amount of information to be extracted from the analysis of biological surfaces than ever before.

Acknowledgments

The authors thank Dr. Chuanbin Mao (University of Oklahoma) for providing the mouse brain samples; Dr. Mao is grateful for the financial support from the National Institutes of Health (1R21EB015190). This research was supported by grants from the Research Council of the University of Oklahoma Norman Campus, the American Society for Mass Spectrometry Research Award (sponsored by Waters Corporation), Oklahoma Center for the Advancement of Science and Technology (grant HR 14−152), and National Institutes of Health (R01GM116116).

References

1. Ye, H., Gemperline, E., Li, L.: A vision for better health: mass spectrometry imaging for clinical diagnostics. Clin. Chim. Acta **420**, 11–22 (2013)
2. Schwamborn, K.: Imaging mass spectrometry in biomarker discovery and validation. J. Proteome. **75**, 4990–4998 (2012)
3. Spengler, B.: Mass spectrometry imaging of biomolecular information. Anal. Chem. **87**, 64–82 (2015)
4. Hsu, C.C., Dorrestein, P.C.: Visualizing life with ambient mass spectrometry. Curr. Opin. Biotechnol. **31**, 24–34 (2015)
5. Takats, Z., Wiseman, J.M., Gologan, B., Cooks, R.G.: Mass spectrometry sampling under ambient conditions with desorption electrospray ionization. Science **306**, 471–473 (2004)
6. Wu, C., Dill, A.L., Eberlin, L.S., Cooks, R.G., Ifa, D.R.: Mass spectrometry imaging under ambient conditions. Mass Spectrom. Rev. **32**, 218–243 (2013)
7. Angel, P.M., Caprioli, R.M.: Matrix-Assisted laser desorption ionization imaging mass spectrometry: in situ molecular mapping. Biochemistry **52**, 3818–3828 (2013)
8. Kraft, M.L., Klitzing, H.A.: Imaging lipids with secondary ion mass spectrometry. Biochim. Biophys. Acta **1841**, 1108–1119 (2014)
9. Rompp, A., Spengler, B.: Mass spectrometry imaging with high resolution in mass and space. Histochem. Cell. Biol. **139**, 759–783 (2013)
10. Yang, J.H., Caprioli, R.M.: Matrix sublimation/recrystallization for imaging proteins by mass spectrometry at high spatial resolution. Anal. Chem. **83**, 5728–5734 (2011)
11. Bich, C., Havelund, R., Moellers, R., Touboul, D., Kollmer, F., Niehuis, E., Gilmore, I.S., Brunelle, A.: Argon cluster ion source evaluation on lipid standards and rat brain tissue samples. Anal. Chem. **85**, 7745–7752 (2013)
12. Nemes, P., Woods, A.S., Vertes, A.: Simultaneous imaging of small metabolites and lipids in rat brain tissues at atmospheric pressure by laser ablation electrospray ionization mass spectrometry. Anal. Chem. **82**, 982–988 (2010)
13. Ovchinnikova, O.S., Bhandari, D., Lorenz, M., Van Berkel, G.J.: Transmission geometry laser ablation into a non-contact liquid vortex capture probe for mass spectrometry imaging. Rapid Commun. Mass Spectrom. **28**, 1665–1673 (2014)
14. Shrestha, B., Vertes, A.: In situ metabolic profiling of single cells by laser ablation electrospray ionization mass spectrometry. Anal. Chem. **81**, 8265–8271 (2009)
15. Beach, D.G., Walsh, C.M., McCarron, P.: High-throughput quantitative analysis of domoic acid directly from mussel tissue using laser ablation electrospray ionization-tandem mass spectrometry. Toxicon **92**, 75–80 (2014)
16. Ifa, D.R., Wu, C., Ouyang, Z., Cooks, R.G.: Desorption electrospray ionization and other ambient ionization methods: current progress and preview. Analyst **135**, 669–681 (2010)
17. Tata, A., Perez, C.J., Hamid, T.S., Bayfield, M.A., Ifa, D.R.: Analysis of metabolic changes in plant pathosystems by imprint imaging DESI-MS. J. Am. Soc. Mass Spectrom. **26**, 641–648 (2015)
18. Eberlin, L.S., Ferreira, C.R., Dill, A.L., Ifa, D.R., Cooks, R.G.: Desorption electrospray ionization mass spectrometry for lipid characterization and biological tissue imaging. BBA-Mol. Cell. Biol. Lipids **1811**, 946–960 (2011)
19. Gerbig, S., Golf, O., Balog, J., Denes, J., Baranyai, Z., Zarand, A., Raso, E., Timar, J., Takats, Z.: Analysis of colorectal adenocarcinoma tissue by desorption electrospray ionization mass spectrometric imaging. Anal. Bioanal. Chem. **403**, 2315–2325 (2012)
20. Campbell, D.I., Ferreira, C.R., Eberlin, L.S., Cooks, R.G.: Improved spatial resolution in the imaging of biological tissue using desorption electrospray ionization. Anal. Bioanal. Chem. **404**, 389–398 (2012)
21. Rao, W., Celiz, A.D., Scurr, D.J., Alexander, M.R., Barrett, D.A.: Ambient DESI and LESA-MS analysis of proteins adsorbed to a biomaterial surface using in-situ surface tryptic digestion. J. Am. Soc. Mass Spectrom. **24**, 1927–1936 (2013)
22. Van Berkel, G.J., Sanchez, A.D., Quirke, J.M.: Thin-layer chromatography and electrospray mass spectrometry coupled using a surface sampling probe. Anal. Chem. **74**, 6216–6223 (2002)
23. Van Berkel, G.J., Ford, M.J., Doktycz, M.J., Kennel, S.J.: Evaluation of a surface-sampling probe electrospray mass spectrometry system for the analysis of surface-deposited and affinity-captured proteins. Rapid Commun. Mass Spectrom. **20**, 1144–1152 (2006)
24. Kertesz, V., Van Berkel, G.J.: Fully automated liquid extraction-based surface sampling and ionization using a chip-based robotic nanoelectrospray platform. J. Mass Spectrom. **45**, 252–260 (2010)
25. Edwards, R.L., Creese, A.J., Baumert, M., Griffiths, P., Bunch, J., Cooper, H.J.: Hemoglobin variant analysis via direct surface sampling of dried blood spots coupled with high-resolution mass spectrometry. Anal. Chem. **83**, 2265–2270 (2011)
26. Quanico, J., Franck, J., Dauly, C., Strupat, K., Dupuy, J., Day, R., Salzet, M., Fournier, I., Wisztorski, M.: Development of liquid microjunction extraction strategy for improving protein identification from tissue sections. J. Proteome. **79**, 200–218 (2013)

27. Prideaux, B., ElNaggar, M.S., Zimmerman, M., Wiseman, J.M., Li, X., Dartois, V.: Mass spectrometry imaging of levofloxacin distribution in TB-infected pulmonary lesions by MALDI-MSI and continuous liquid microjunction surface sampling. Int. J. Mass Spectrom. **377**, 699–708 (2015)
28. Roach, P.J., Laskin, J., Laskin, A.: Nanospray desorption electrospray ionization: an ambient method for liquid-extraction surface sampling in mass spectrometry. Analyst **135**, 2233–2236 (2010)
29. Laskin, J., Heath, B.S., Roach, P.J., Cazares, L., Semmes, O.J.: Tissue imaging using nanospray desorption electrospray ionization mass spectrometry. Anal. Chem. **84**, 141–148 (2012)
30. Lanekoff, I., Thomas, M., Carson, J.P., Smith, J.N., Timchalk, C., Laskin, J.: Imaging nicotine in rat brain tissue by use of nanospray desorption electrospray ionization mass spectrometry. Anal. Chem. **85**, 882–889 (2013)
31. Lanekoff, I., Geydebrekht, O., Pinchuk, G.E., Konopka, A.E., Laskin, J.: Spatially resolved analysis of glycolipids and metabolites in living *Synechococcus* sp PCC 7002 using nanospray desorption electrospray ionization. Analyst **138**, 1971–1978 (2013)
32. Lanekoff, I., Burnum-Johnson, K., Thomas, M., Short, J., Carson, J.P., Cha, J., Dey, S.K., Yang, P., Prieto Conaway, M.C., Laskin, J.: High-speed tandem mass spectrometric in situ imaging by nanospray desorption electrospray ionization mass spectrometry. Anal. Chem. **85**, 9596–9603 (2013)
33. Rao, W., Pan, N., Yang, Z.: High resolution tissue imaging using the single-probe mass spectrometry under ambient conditions. J. Am. Soc. Mass Spectrom. **26**, 986–993 (2015)
34. Pan, N., Rao, W., Kothapalli, N.R., Liu, R., Burgett, A.W., Yang, Z.: The single-probe: a miniaturized multifunctional device for single cell mass spectrometry analysis. Anal. Chem. **86**, 9376–9380 (2014)
35. Cech, N.B., Enke, C.G.: Practical implications of some recent studies in electrospray ionization fundamentals. Mass Spectrom. Rev. **20**, 362–387 (2001)
36. Laskin, J., Eckert, P.A., Roach, P.J., Heath, B.S., Nizkorodov, S.A., Laskin, A.: Chemical analysis of complex organic mixtures using reactive nanospray desorption electrospray ionization mass spectrometry. Anal. Chem. **84**, 7179–7187 (2012)
37. Jackson, A.U., Shum, T., Sokol, E., Dill, A., Cooks, R.G.: Enhanced detection of olefins using ambient ionization mass spectrometry: Ag^+ adducts of biologically relevant alkenes. Anal. Bioanal. Chem. **399**, 367–376 (2011)
38. Dodbiba, E., Xu, C., Payagala, T., Wanigasekara, E., Moon, M.H., Armstrong, D.W.: Use of ion pairing reagents for sensitive detection and separation of phospholipids in the positive ion mode LC-ESI-MS. Analyst **136**, 1586–1593 (2011)
39. Chu, S.G., Chen, D., Letcher, R.J.: Dicationic ion-pairing of phosphoric acid diesters post-liquid chromatography and subsequent determination by electrospray positive ionization-tandem mass spectrometry. J. Chromatogr. A **1218**, 8083–8088 (2011)
40. Xu, C., Armstrong, D.W.: High-performance liquid chromatography with paired ion electrospray ionization (PIESI) tandem mass spectrometry for the highly sensitive determination of acidic pesticides in water. Anal. Chim. Acta **792**, 1–9 (2013)
41. Rao, W., Mitchell, D., Licence, P., Barrett, D.A.: The use of dicationic ion-pairing compounds to enhance the ambient detection of surface lipids in positive ionization mode using desorption electrospray ionisation mass spectrometry. Rapid Commun. Mass Spectrom. **28**, 616–624 (2014)
42. Lostun, D., Perez, C.J., Licence, P., Barrett, D.A., Ifa, D.R.: Reactive DESI-MS imaging of biological tissues with dicationic ion-pairing compounds. Anal. Chem. **87**, 3286–3293 (2015)
43. Lanekoff, I., Heath, B.S., Liyu, A., Thomas, M., Carson, J.P., Laskin, J.: Automated platform for high-resolution tissue imaging using nanospray desorption electrospray ionization mass spectrometry. Anal. Chem. **84**, 8351–8356 (2012)
44. Thomas, M., Heath, B.S., Laskin, J., Li, D.S., Liu, E., Hui, K., Kuprat, A.P., van Dam, K.K., Carson, J.P.: Visualization of High Resolution Spatial Mass Spectrometric Data during Acquisition. Proceedings of the 2012 Annual International Conference of the IEEE Engineering in Medicine and Biology Society (EMBC), pp. 5545–5548. San Diego, CA, USA, 28 Aug-01 Sep. (2012)
45. Nielen, M.W., van Beek, T.A.: Macroscopic and microscopic spatially-resolved analysis of food contaminants and constituents using laser-ablation electrospray ionization mass spectrometry imaging. Anal. Bioanal. Chem. **406**, 6805–6815 (2014)
46. Girod, M., Shi, Y., Cheng, J.X., Cooks, R.G.: Mapping lipid alterations in traumatically injured rat spinal cord by desorption electrospray ionization imaging mass spectrometry. Anal. Chem. **83**, 207–215 (2011)
47. Girod, M., Shi, Y., Cheng, J.X., Cooks, R.G.: Desorption electrospray ionization imaging mass spectrometry of lipids in rat spinal cord. J. Am. Soc. Mass Spectrom. **21**, 1177–1189 (2010)
48. Luxembourg, S.L., Mize, T.H., McDonnell, L.A., Heeren, R.M.: High-spatial resolution mass spectrometric imaging of peptide and protein distributions on a surface. Anal. Chem. **76**, 5339–5344 (2004)
49. Xu, C., Armstrong, D.W.: High-performance liquid chromatography with paired ion electrospray ionization (PIESI) tandem mass spectrometry for the highly sensitive determination of acidic pesticides in water. Anal. Chim. Acta **792**, 1–9 (2013)
50. Xu, C., Guo, H., Breitbach, Z.S., Armstrong, D.W.: Mechanism and sensitivity of anion detection using rationally designed unsymmetrical dications in paired ion electrospray ionization mass spectrometry. Anal. Chem. **86**, 2665–2672 (2014)
51. Greer, T., Sturm, R., Li, L.: Mass spectrometry imaging for drugs and metabolites. J. Proteome. **74**, 2617–2631 (2011)